Fermi National Accelerator Laboratory

FERMILAB-Conf-92/66

Operation and Radiation Resistance of a FOXFET Biasing Structure for Silicon Strip Detectors

M. Laakso, Particle Detector Group

Fermi National Accelerator Laboratory
P.O. Box 500, Batavia, Illinois 60510
Research Institute for High Energy Physics (SEFT)
Helsinki, Finland

P. Singh, E. Engels, Jr., P. Shepard

Department of Physics and Astronomy
University of Pittsburgh, Pittsburgh, PA

February 1992

Submitted to the *Sixth European Symposium on Semiconductor Detectors*, Milano, Italy, February 24-27, 1992.

Disclaimer

OPERATION AND RADIATION RESISTANCE OF A FOXFET BIASING STRUCTURE FOR SILICON STRIP DETECTORS

M. Laakso
Particle Detector Group, Fermilab, Batavia, Illinois, USA and
Research Institute for High Energy Physics (SEFT), Helsinki, Finland

P. Singh, E. Engels, Jr., P.F. Shepard
Department of Physics and Astronomy,
University of Pittsburgh, Pittsburgh, PA, USA

Abstract

AC-coupled strip detectors biased with a FOXFET transistor structure have been studied. Measurement results for the basic operational characteristics of the FOXFET are presented together with a brief description of the physics underlying its operation.

Radiation effects were studied using photons from a ^{137}Cs source. Changes in the FOXFET characteristics as a function of radiation dose up to 1 MRad are reported. Results about the effect of radiation on the noise from a FOXFET biased detector are described.

Submitted to Sixth European Symposium on Semiconductor Detectors,
Milano 24. - 27.2.1992

1. Introduction

Silicon microstrip detectors for high-precision charged particle position measurements have been used in nuclear and particle physics for years. The detectors have evolved from simple surface barrier strip detectors with metal strips [1] to highly complicated double-sided AC-coupled junction detectors [2]. AC-coupling the readout electrodes from the diode strips necessitates a separate biasing structure for the strips. A suitable biasing structure consists of a common bias line together with a means for preventing the signal from one strip from spreading to its neighbours through the bias line. One solution to this is to bias the strips through appropriate value resistors, which can be integrated on the detector wafer as polysilicon resistors [3].To circumvent the extra processing step required for polysilicon resistor processing and the problem of obtaining uniform and high enough resistance values throughout the large detector area, alternative methods for strip biasing have been devised. These include the usage of electron accumulation layer resistance for n^+- strips [4], and the usage of the phenomenon known as the punch-through effect for p^+- strips [5,6]. In this paper we present measurement results about the operation and radiation resistance of detectors utilizing a punch-through effect biasing structure known as a Field OXide Field-Effect Transistor (FOXFET) [7].

2. The punch-through effect

The operation of the FOXFET biasing structure is based on the punch-through effect previously reported in the context of p^+np^+ diodes for microwave applications [8]. When a voltage is applied between the p^+ regions in a p^+np^+

structure, the voltage is divided between the two pn junctions. Hence one of the junctions becomes forward biased and the other one reverse biased. At low applied voltages the voltage sharing is determined by the condition that the current flowing through both junctions be the same, which means that most of the voltage is carried by the reverse biased junction (RB) and only a minor fraction by the forward biased junction (FB). When the depletion region produced by the RB junction meets the shallow depletion region of the FB junction, a punch-through (reach-through) is said to occur, and the current through the device starts to be dominated by the hole current thermionically emitted over the FB junction. The current flowing through the device increases exponentially as a function of voltage over the FB junction after punch-through is reached.

3. The FOXFET structure

A FOXFET structure used for silicon microstrip detector biasing is depicted in fig. 1, which shows a cross section of the detector in the direction of the strips. In the design a p^+ diffusion (bias line) has been placed close (5-10μm) to the ends of the p^+ diode strips to be biased. The aluminum gate electrode of the FOXFET is on top of the field oxide between the bias line and the ends of the strips. Thus, the design is a multi-source MOS transistor where the bias line (i.e. the drain of the transistor) and the gate are common, and each strip acts as an individual source. The silicon part of the FOXFET can also be thought of as a lateral p^+np^+ diode, and in a qualitative analysis can be treated analogously. However, in quantifying the relevant parameters describing its operation the surface effects caused by the positive charge in the field oxide are important and have to be taken into account.

In detector operation the bias line is grounded and a positive bias voltage is applied to the back of the detector. The purpose of the p^+np^+ structure is to reach

a punch-through condition when the voltage difference between the strips and the bias line exceeds a maximum value defined by the geometry and bias conditions of the FOXFET. This way the strip potential is held close to the potential of the grounded bias line, and an effective bias voltage exists between the strips and the backplane. A negative gate voltage can be applied to control the operation of the FOXFET.

4. Results

4.1 General

The detectors used in the measurements[1] were single-sided strip detectors manufactured on a high-resistivity (≈10 kΩcm) 300 μm thick wafer. The detector area of 85 x 24 mm was divided into 384 strips on a 60 μm pitch. The gate length of the FOXFET structures used for biasing was 6 μm, and the oxide thickness 1 μm. The detectors were mounted on test PC boards, and connections to the appropriate contacts (gate, bias line, guard ring, two DC connections to different strips) were made with ultrasonic wire bonding. Contact to the back of the detector was made with conductive epoxy.

The DC measurements reported were made with a programmable multichannel source-monitor unit[2]. To avoid the effect of varying ambient humidity, the measurements were made with the detector in a dry N_2 environment.

For radiation damage measurements the detectors were irradiated with ^{137}Cs 667 keV photons at the University of Pittsburgh. The dose rate delivered by the

---

[1] Manufactured by Micron Semiconductor Ltd., Lancing, Sussex, England

[2] Type Hewlett Packard 4145B

source at the detector location was 156 kRad/hr, 274 kRad/hr or 366 kRad/hr as measured with a calibrated air-ionisation chamber. The detector was placed in the radiation field facing the source with no material in between. The gate voltage was held at - 9V during irradiation, the electric field in the oxide being $\approx 9 \cdot 10^4 \frac{V}{cm}$. The cumulative radiation doses given to the detectors were 10 kRad, 20 kRad, 50 kRad, 100 kRad, 500 kRad and 1 MRad. The reported DC measurements were made typically 24 hours after irradiation, during which time the detector was shipped from Pittsburgh to Fermilab. The time between irradiations was approximately 1 week, except for a 100 d interval between 100 kRad and 500 kRad irradiations on one of the detectors.

4.2 Results

4.2.1 Initial conditions

We start by describing the conditions in the FOXFET before any voltages are applied. The field (also FOXFET gate) oxide contains positive oxide charge of different types [9], the density of which is typically 10^{11}-10^{12} cm^{-2}. This oxide charge induces an electron accumulation layer under the oxide. The excess electron concentration in this induced layer can be found by solving the Poisson equation in the surface region with the assumption that the space charge from donor ions can be neglected, and stating that the total amount of excess electrons should equal the oxide charge density [10]. The p^+ contacts create a depletion region around themselves through the natural built-in voltage in the pn-junction. In 10 kΩ-cm silicon, the thickness of this built-in depletion region is ≈ 45 μm, so

the part of the silicon surrounding the FOXFET except for the accumulation region under the oxide is depleted already with no bias applied.

4.2.2 Detector leakage current

The detector leakage current increased during irradiations from 87 nA to 1700 nA at 1 MRad. This corresponds to a damage constant of 2.7 $\frac{nA}{cm^3 kRad}$, which is in agreement with previous studies done with non-hadronic irradiation [11]. The leakage current increase due to photon irradiation is not very significant compared with the effects due to the buildup of charge in the field oxide of the detector. The leakage current increase from an equivalent dose of hadronic radiation would be much greater.

4.2.3 Strip voltage characteristics

Fig. 2 shows the measured strip voltage as a function of bias voltage applied to the back of the detector. The input impedance of the voltage measuring instrument was $>10^{12}\ \Omega$, which ensures that the strip voltage was not affected by the measurement. The strip voltage shows a typical behavior of first increasing with the bias voltage, then settling to the punch-through voltage, which is controlled by the voltage on the gate. In a simple picture the strips are at low bias voltages fully floating, and should follow the bias voltage exactly (with the difference of the built-in voltage in the pn junction) until punch-through occurs, after which the strip voltage should be constant. The observed deviation from this behaviour is caused by the requirement for the detector leakage current and

FOXFET current before punch-through to be the same, which leads to voltage sharing between the strip junction and the FOXFET.

The punch-through voltage for V_g=0 is approximately 11 V, which may be compared with a calculated value of 10 mV for punch-through between two p^+ regions with 6 μm of 10 kΩcm n-type silicon in between, with no surface effects involved. Obviously the accumulation layer really effectively inhibits the punch-through at the surface. At more negative gate voltages V_{pt} gets smaller, as the gate voltage partly compensates the effect of the positive oxide charge in creating the electron accumulation layer. At gate voltage V_g = -22V V_{pt} is zero, which indicates that the accumulation layer has vanished and that the transistor is starting to turn on.

The total amount of oxide charge present can be estimated by noting that at gate voltage = -22V the charge on the gate equals the oxide charge. This gives an oxide charge of ≈ 5 10^{11} 1/cm^2.

The effect of radiation on the FOXFET structure is well illustrated by fig. 3, which depicts the strip voltage (punch-through voltage) as a function of gate voltage for different radiation doses. Both the punch-through voltage and the transistor threshold voltage increase quickly at doses up to 20 kRad, after which the rate of change is much smaller and the voltages tend to saturate. The threshold voltage shift observed at 100 kRad is 14.5 V. During the 100 d period between 100 kRad and 500 kRad irradiations the detector annealed significantly, so that the threshold and punch-through voltages after the 500 kRad and 1 MRad doses actually remain lower than at 100 kRad after annealing. In the case of a second detector, which was not stored between irradiations, increase in punch-through voltage vs. dose was monotonic.

The increase in the punch-through voltage and the FOXFET threshold voltage can be understood in the framework explained in section 4.2.1, where the oxide

charge induced electron accumulation layer significantly increases punch-through voltage. As the radiation increases the amount of positive charge in the oxide, the electron accumulation layer gets stronger and the punch-through voltage increases. The amount of oxide charge present after irradiation to 100 kRad is (calculated from the threshold voltage) $\approx 8 \cdot 10^{11}$ cm^{-2}. Typically a saturation in oxide charge buildup is reached when oxide charge approaches the value 2.5 - 3.0$\cdot 10^{12}$ cm^{-2}. This, however does not seem to apply in our case. The saturation phenomenon observed in our measurements is explained in the following.

According to the simple theory of radiation induced charge buildup [12] interface charge buildup does not appear if a negative gate voltage is applied during irradiation, since no positive charges are transported to the interface. The effect of charge buildup in thick oxides and under negative gate voltages has been studied by Boesch and co-workers [13], whose results indicate that another mechanism for charge buildup during irradiation does exist, which causes charge buildup at the interface even with negative gate voltages. For irradiations with negative gate voltages, it also holds true that if charge trapping occurs also in the bulk of the oxide (which has been observed for field oxides [12]), the trapped charge starts to perturb the applied electric field when the observed flatband voltage shifts approach the voltage applied to the gate. When that occurs, the electric field at the Si-SiO_2 interface approaches zero and efficient recombination at this low field region suppresses the charge trapping. Hence at low doses charge trapping occurs both at the interface and in the bulk of the oxide, resulting in a quick increase of the oxide charge and consequently punch-through and threshold voltage. When the trapped charge in the bulk of the oxide equals the charge at the gate during irradiation, electric field goes to zero first at the interface, and with increasing charge trapping the zero field recombination region extends inward to the bulk of the oxide. The creation of the zero field region should occur when the

shift in the threshold voltage caused by oxide charge trapping equals the gate voltage during irradiation, which is indeed close to our experimental observation. After the electric field is zero throughout the oxide, only trapping at the interface (created by radiation interactions at the interface region [13]) continues causing the slow increase in the punch-through and threshold voltages.

The annealing process is a tunnel anneal at the Si-SiO_2 interface, where electrons from silicon tunnel to the oxide and recombine with charge trapped at or near the Si-SiO_2 interface. Thus the annealing process does not significantly reduce the amount of charge trapped in the bulk of the oxide, but only that at the interface region. This means that the electric field conditions in the oxide, which led to the saturation of the charge buildup in the oxide, do not change during annealing, although charge from the interface is removed. After annealing charge trapping still only occurs through radiation interactions at the interface and is, therefore, relatively slow.

4.2.4 Current vs. voltage characteristics, dynamic resistance

In operating the detector it is essential for the user to know the I-V characteristics of the strip biasing structure to be able to predict detector behavior with increasing leakage current or damaged strips. For detectors with resistive bias elements the relevant quantity is the resistance value of the bias resistor. For a non-linear biasing element like a FOXFET the situation is not so straightforward.

In the following we have measured the I-V characteristics of a FOXFET structure. This can be done by injecting a current to the FOXFET and measuring the corresponding change in the strip voltage. In addition to injecting the current to one strip using a current source, a measurement was made by increasing the leakage current in the whole detector by shining a controlled amount of light on it.

Fig. 4 illustrates the measurement setup during current injection measurements. The injected current was varied logarithmically from 40 pA to 400 nA, and corresponding changes in the strip voltages were recorded. The strip voltage as a function of injected current for different gate voltages is depicted in fig. 5. Because of the exponential behavior of the current after punch-through, which can be observed from fig. 5, the voltage drop caused by a current of 400 nA/strip is about 0.8 V. Essentially the same behavior was observed by shining controlled amounts of light on the detector and thus increasing the leakage current in a manner better resembling leakage current increase caused by bulk damage (fig. 6). From fig. 5 we can also see that changes in the gate voltage have little effect on the shape of the I-V curve except when the gate voltage approaches the threshold voltage, in this case at voltages exceeding -22 V.

A subject of interest in the FOXFET is the quantity known as the dynamic resistance, defined as:

$$R_d = \frac{\delta V_s}{\delta I_s} \qquad (1)$$

Fig. 7 shows the dynamic resistance as a function of injected current with different gate voltages. The resistance is very high, over 100MΩ, at very low currents, and decreases as a function of injected current to around 1 MΩ at 400 nA. The I-V behavior of the FOXFET can to some approximation be modelled by the forward biased diode equation. In that case the current - voltage characteristics and the dynamic resistance as a function of injected current can be expressed as:

$$I_s = I_0 \left(e^{\beta(V-V_{pt})} - 1\right) \qquad (2)$$

$$R_D = \frac{\delta V}{\delta I} = \frac{1}{\beta(I_s + I_o)} \qquad (3)$$

where V_{pt} = punch-through voltage, $\beta = kT/q$ for an ideal, bulk geometry. I_o can be interpreted as the current flowing through the FOXFET with no external current injected, i.e. the detector leakage current. Thus for currents exceeding I_o the dynamic resistance behaves essentially as I^{-1}. A more accurate analysis [8] takes into account voltage sharing between the forward and reverse biased junctions at the p^+np^+ structure.

Fig. 8 shows the dependence of dynamic resistance on the gate voltage, where we observe the dynamic resistance be relatively weakly dependent on the gate voltage at gate voltages below the threshold voltage V_T. At the threshold voltage a sharp drop in the dynamic resistance is seen, as the transistor is turned on and operates in its linear region.

Fig. 9 shows the measured dynamic resistance as a function of injected current for different radiation doses. The behavior shows the typical I_{inj}^{-1} - dependence at large currents. At low currents the resistance decreases by a factor of 4 at 1 MRad, whereas the dynamic resistance value measured high currents (≈100 nA/strip) shows practically no dependence on dose. This is better illustrated in fig. 10 where the dynamic resistance has been plotted versus radiation dose. The effect at low currents is to a large extent explained by the increase in the leakage current at higher radiation doses. Fig. 10 shows also the expected dynamic resistance decrease calculated using the increased detector leakage current and the measured (fig. 7) dependence of dynamic resistance on current. The strip current used in the calculation is obtained by simply dividing the

total leakage current of the detector by the number of strips, which may account for the small difference between measured and calculated values in fig. 10.

5. Noise performance

The performance as a charged particle detector of one of the two detectors studied was investigated using a ^{106}Ru ß-source. A pulse height spectrum for a single strip is shown in fig. 11. The gate for the pulse height analyzer was generated using a scintillation counter located behind the silicon detector in coincidence with the strip studied. The adjacent strips were placed in anticoincidence to eliminate events where the charge from the electron passing through the detector produced significant sharing with an adjacent strip. The threshold requirement on the strip studied was used to partially suppress the observed noise peak, but was set very low in order to avoid biasing the observed pulse height spectrum. For a 300 micron thick detector the most probable energy loss is 78 keV corresponding to 21700 electron-hole pairs. The channel separation between the noise peak and the peak of the electron spectrum provides an energy calibration for the spectrum and permits a measurement of the noise by converting the width of the observed noise peak in channels to an equivalent noise charge (ENC). In this case the observed noise was about 840 electrons.

We studied the observed noise and pulse height spectrum as a function of the gate-drain voltage applied to the FOXFET before irradiation with ^{137}Cs and after an exposure of 600 kRads. These data are shown in fig. 12. The noise is essentially the same before and after irradiation and independent of the gate-drain voltage for normal operation of the FOXFET in its subthreshold region. The onset of increased noise at about -22 V before irradiation and approximately -32 V after 600 kRads is due to the turning on of the FOXFET and the resultant sharp drop in

its dynamic resistance. The most obvious effect is the shift in the FOXFET threshold due to the build up of charge under the gate of the FOXFET, as described in the previous section.

The noise behaviour of the detector as a function of the leakage current was also investigated. To duplicate the large leakage currents which are produced by hadronic damage to the bulk of the detector, the detector was exposed to light. This was previously shown in fig. 6. Fig. 6 shows the total leakage current through the FOXFET produced by different light levels versus the source-drain or punch-through voltage. Two different gate-drain voltages are shown both before irradiation and after exposure to 100 kRads. There is relative little change in the punch-through voltage as the leakage current increases. The major effect is the shift in the punch through voltage as a result of the irradiation of the FOXFET.

A concern is that at very large leakage currents the dynamic resistance of the FOXFET will become too small to collect the charge from the passage of a charged particle and also give rise to extra noise in addition to the shot noise associated with the leakage current. A measurement of the noise versus leakage current for the entire detector is shown in fig. 13. Since the detector has 384 strips, the maximum leakage current of 400 μA corresponds to a leakage current in excess of one μA per strip. The curve through the data is a calculation of the shot noise from the leakage current added in quadrature with the amplifier noise determined at low leakage currents. The calculation assumed CR-RC shaping with a peaking time of 0.25 microseconds. The base amplifier noise was 840 electrons. The data indicates that there is no discernable increase in the noise from the decreasing resistance of the FOXFET as the leakage current is increased.

6. Conclusions

The behavior of a FOXFET strip detector biasing structure can be well understood in the framework of theory for p^+np^+ punch-through structures by taking into account the effect of the positive oxide charge in the FOXFET gate oxide and the FOXFET geometry. The dynamic resistance of the FOXFET varies approximately as I_{ds}^{-1}, and decreases from 80 MΩ at I_{ds}=1 nA to 1MΩ at I_{ds}≈300 nA. The effects of photon irradiation up to 1 MRad on the FOXFET can be qualitatively explained by charge trapping and annealing in the FOXFET gate oxide. A significant annealing of the detector was observed during 100 days storage in room temperature. The FOXFET biasing structure was found to be stable in terms of noise and DC characteristics for doses up to 1 MRad. The significant changes in the FOXFET characteristics were the increase in the punch-through voltage and the threshold voltage due to irradiation. The dynamic resistance of the FOXFET was found to decrease by a factor of 4 after 1 MRad, which was in accordance with the increase of the detector leakage current. No increase in the noise charge at the amplifier input was observed for normal subthreshold operation of the FOXFET for exposures up to 1 MRad. Furthermore, no extra noise due to the decreased dynamic resistance of the FOXFET was observed for leakage currents up to 1 μA per strip.

Acknowledgements

The authors would like to thank F. Bedeschi and C. Haber for useful discussions, R. Yarema for the possibility to use facilities and instruments at the Fermilab Detector Electronics group and K. Bohner for his help in using the ^{137}Cs source at the University of Pittsburgh.

References

[1] England, J.B.A. et. al., "Capacitative Charge Division Read-out with a Silicon Strip Detector", NIM 185(1981) 43-47.

[2] Brenner, R. et. al., "Double-sided Capacitively Coupled Silicon Strip Detectors on a 100 mm Wafer", Proceedings of the IEEE Nuclear Science Symposium, Santa Fe, NM, USA, 1991.
Batignani G. et. al., "Double-Sided Readout Silicon Strip Detectors for the ALEPH Minivertex", NIM A277(1989) 147-153.
Becker H. et. al., "New Developments in Double Sided Silicon Strip Detectors, IEEE Trans. Nucl. Sci, Vol. 37, No. 2, 1990.

[3] Caccia M. et. al., "A Si Strip Detector with Integrated Coupling Capacitors", NIM A260(1987) 124-131.

[4] Becker H. et. al. , ref. 2.

[5] Ellison J. et. al., "Punch-through Currents and Floating Strip Potentials in

Silicon Detectors", IEEE Trans Nucl. Sci., Vol. 36, No. 1, 1989.

[6] Tajima H. et. al., "Utilization of MOS Gate Structure for Capacitive Charge Division Readout of Silicon Strip Detectors", NIM A288 (1990) 536 - 540.

[7] Allport P. et. al., "FOXFET Biassed Microstrip Detectors", NIM A310 (1991) 155 - 159.

[8] Chu, J.L. et. al., "Thermionic Injection and Space-Charge-Limited Current in Reach-Through p^+np^+ Structures", J. Appl. Phys. 43 (1972) 63.

[9] Sze, S.M., "Physics of Semiconductor Devices" 2nd ed., J. Wiley & Sons, 1981.

[10] Muller R.S., Kamins T.I., "Device Electronics for Integrated Circuits" 2nd ed., J. Wiley & Sons, 1986.

[11] Dijkstra H. et. al., "Radiation Hardness of Si Strip Detectors with Integrated Coupling Capacitors", IEEE Trans. Nucl. Sci Vol. 36, No 1, 1989.

[12] Boesch H.E. et. al., "Hole Transport and Trapping in Field Oxides", IEEE Trans. Nucl. Sci. Vol. 32, No. 6, 1985.

[13] Boesch H.E. et. al., "Interface-state Generation in Thick SiO_2 Layers", IEEE Trans. Nucl. Sci., Vol. 29, No. 8, 1982.

Figure captions:

Figure 1. A cross-section along the direction of the strips of the FOXFET structure.

Figure 2. The strip voltage as a function of the bias voltage at the back of the detector.

Figure 3. The strip voltage as a function of gate voltage after different radiation doses with V_{bias} = 35V. Note the annealing, which has occurred during the 100 day period between 100 kRad and 500 kRad irradiations.

Figure 4. Measurement setup during V-I measurements.

Figure 5. FOXFET V-I characteristics. The shape of the V-I curve remains unchanged with different gate voltages until the threshold voltage is reached.

Figure 6. Total leakage current (384 strips) versus punch-through voltage for two different gate-drain voltages before and after 100 kRad of radiation. The leakage current is generated by exposing the detector to light.

Figure 7. Dynamic resistance as a function of current flowing through the FOXFET. The resistance is inversely proportional to the current.

Figure 8. Dynamic resistance as a function of FOXFET gate voltage. The resistance is relatively insensitive to gate voltage until threshold voltage is reached.

Figure 9. Dynamic resistance as a function of current at different radiation doses. Changes at low currents are largely due to increased leakage current at high doses.

Figure 10. Dynamic resistance as a function of dose. No significant change is observed other than that caused by the leakage current increase.

Figure 11. Pulse height spectrum from ^{106}Ru ß-source on a single strip. The signal peak corresponds to an energy deposition of 78 keV or 21700 electron-hole pairs. The width of the noise peak is 840 electrons.

Figure 12. ENC versus gate-drain voltage. The noise is flat and independent of radiation exposure in the subthreshold region of the FOXFET. The noise increases sharply at the threshold of the FOXFET. The threshold is shifted as a result of radiation.

Figure 13. ENC versus total leakage current (384 strips). The smooth curve is a calculation of the shot noise added in quadrature to the amplifier noise.

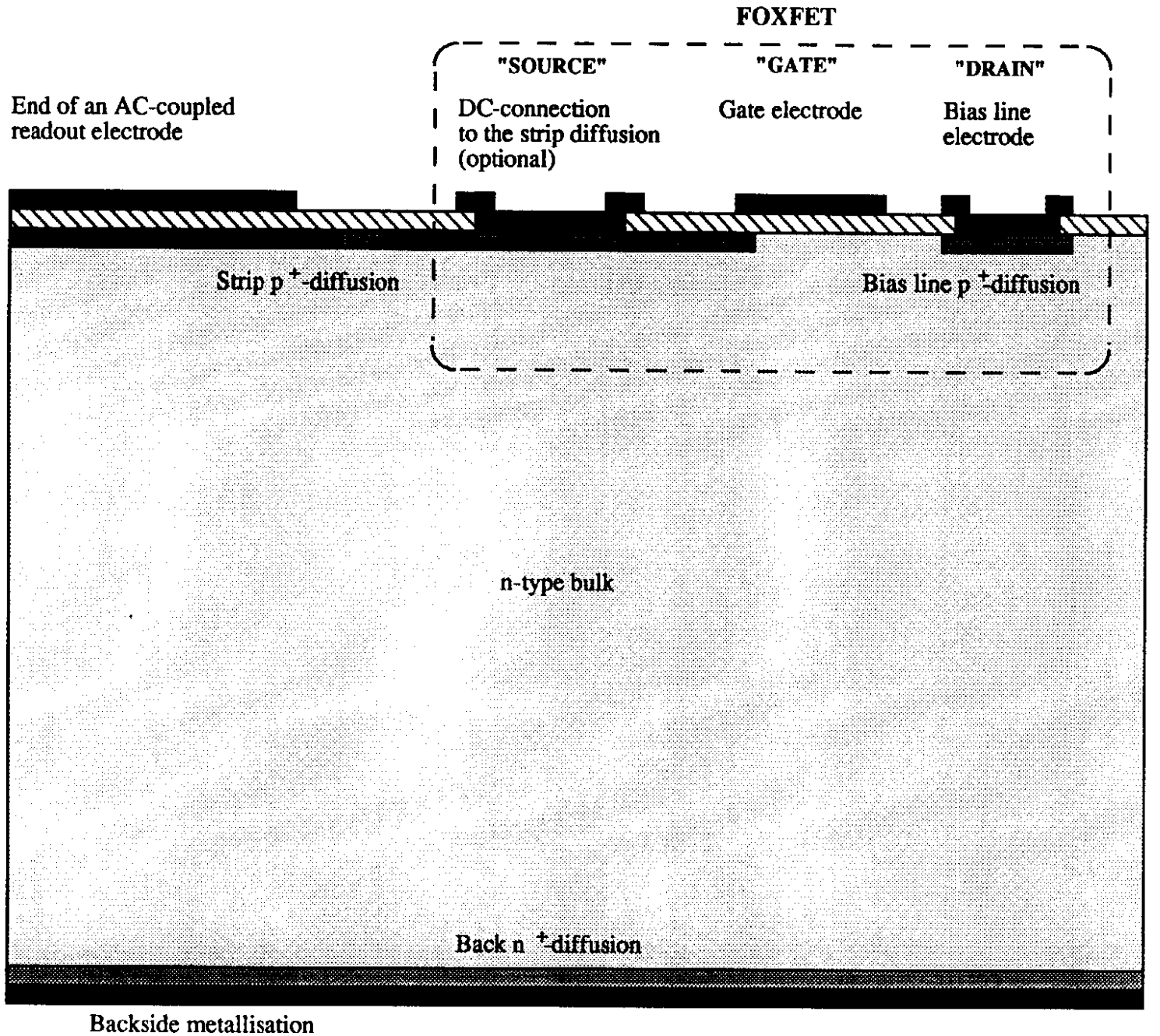
FOXFET
"SOURCE"
"GATE"
"DRAIN"
End of an AC-coupled readout electrode
DC-connection to the strip diffusion (optional)
Gate electrode
Bias line electrode
Strip p+-diffusion
Bias line p+-diffusion
n-type bulk
Back n+-diffusion
Backside metallisation

Fig. 1

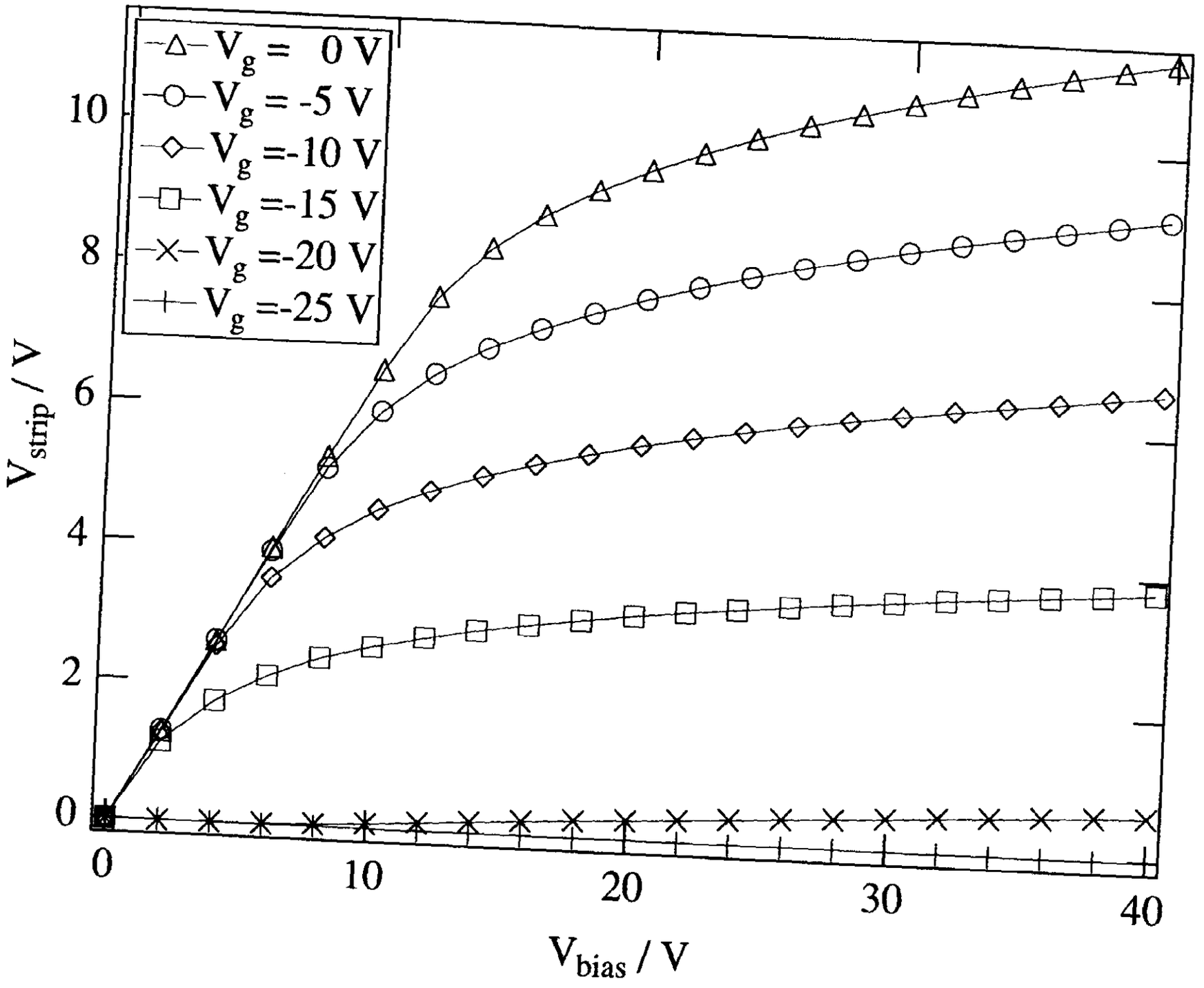
V_g = 0 V
V_g = -5 V
V_g =-10 V
V_g =-15 V
V_g =-20 V
V_g =-25 V
V_{strip} / V
V_{bias} / V
0
2
4
6
8
10
0
10
20
30
40

FIG. 2

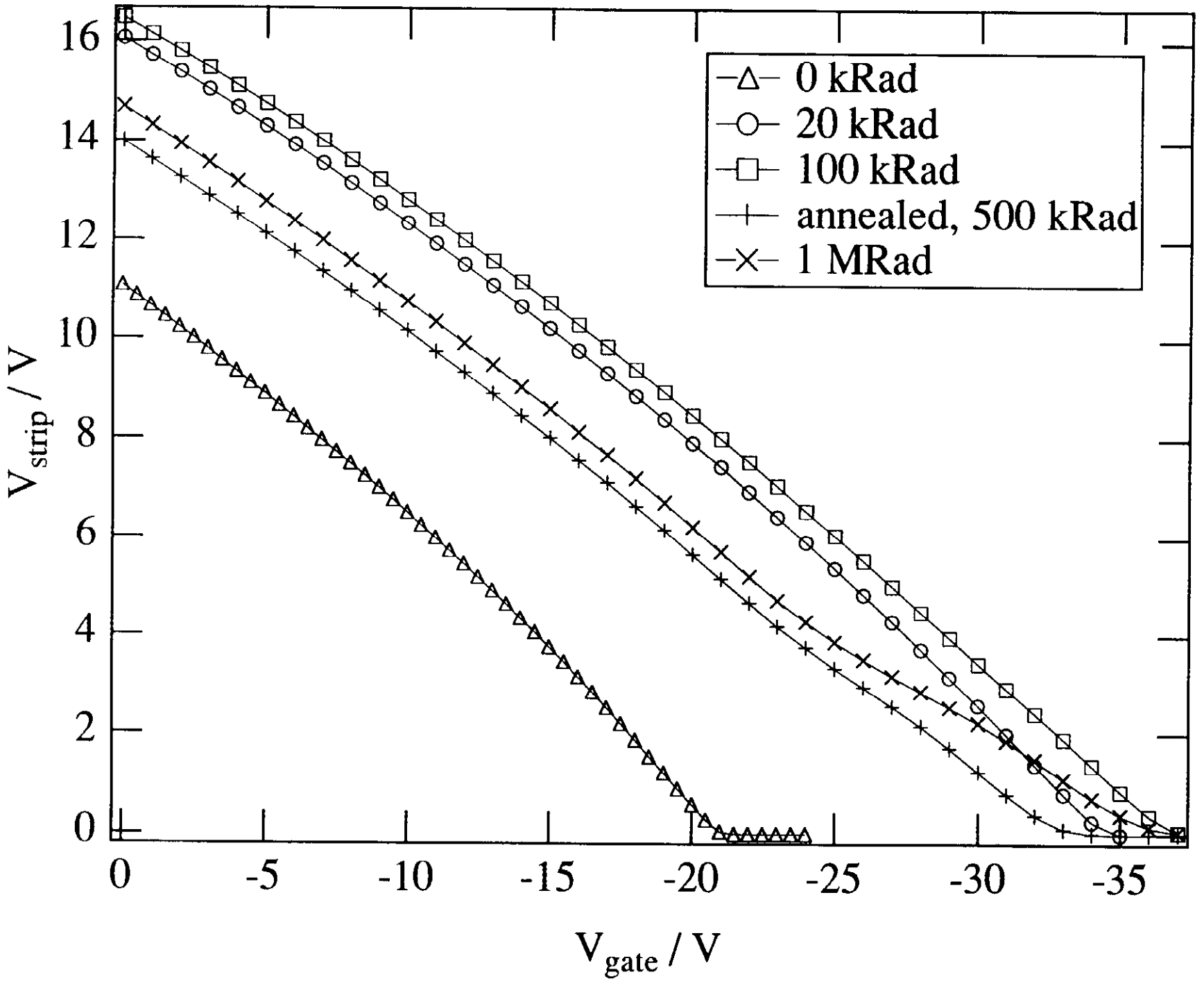
0 kRad
20 kRad
100 kRad
annealed, 500 kRad
1 MRad
V_{strip} / V
V_{gate} / V
16
14
12
10
8
6
4
2
0
0
-5
-10
-15
-20
-25
-30
-35

FIG. 3

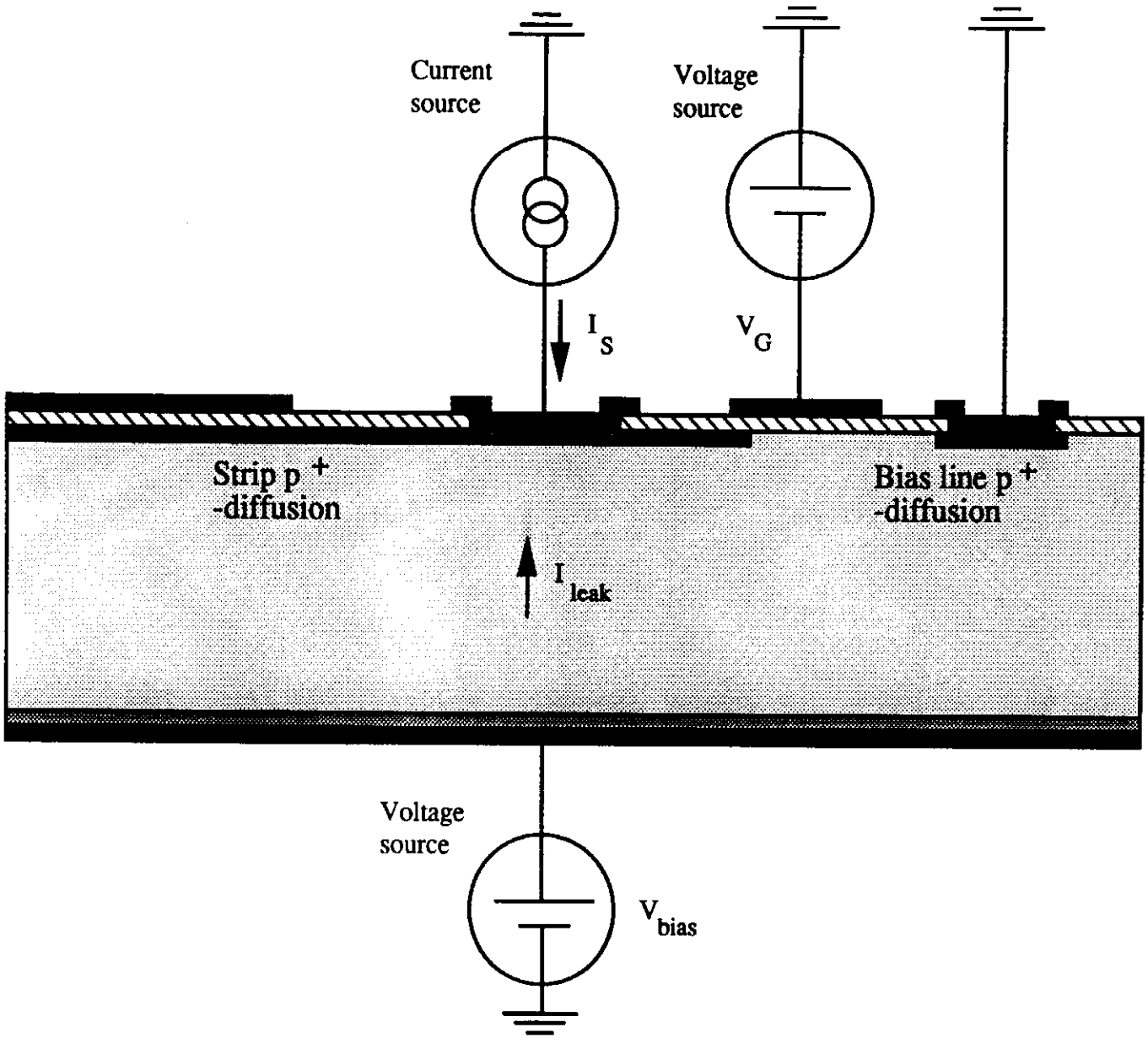
Current
source
Voltage
source
I_S
V_G
Strip p $^+$
-diffusion
Bias line p $^+$
-diffusion
I_{leak}
Voltage
source
V_{bias}

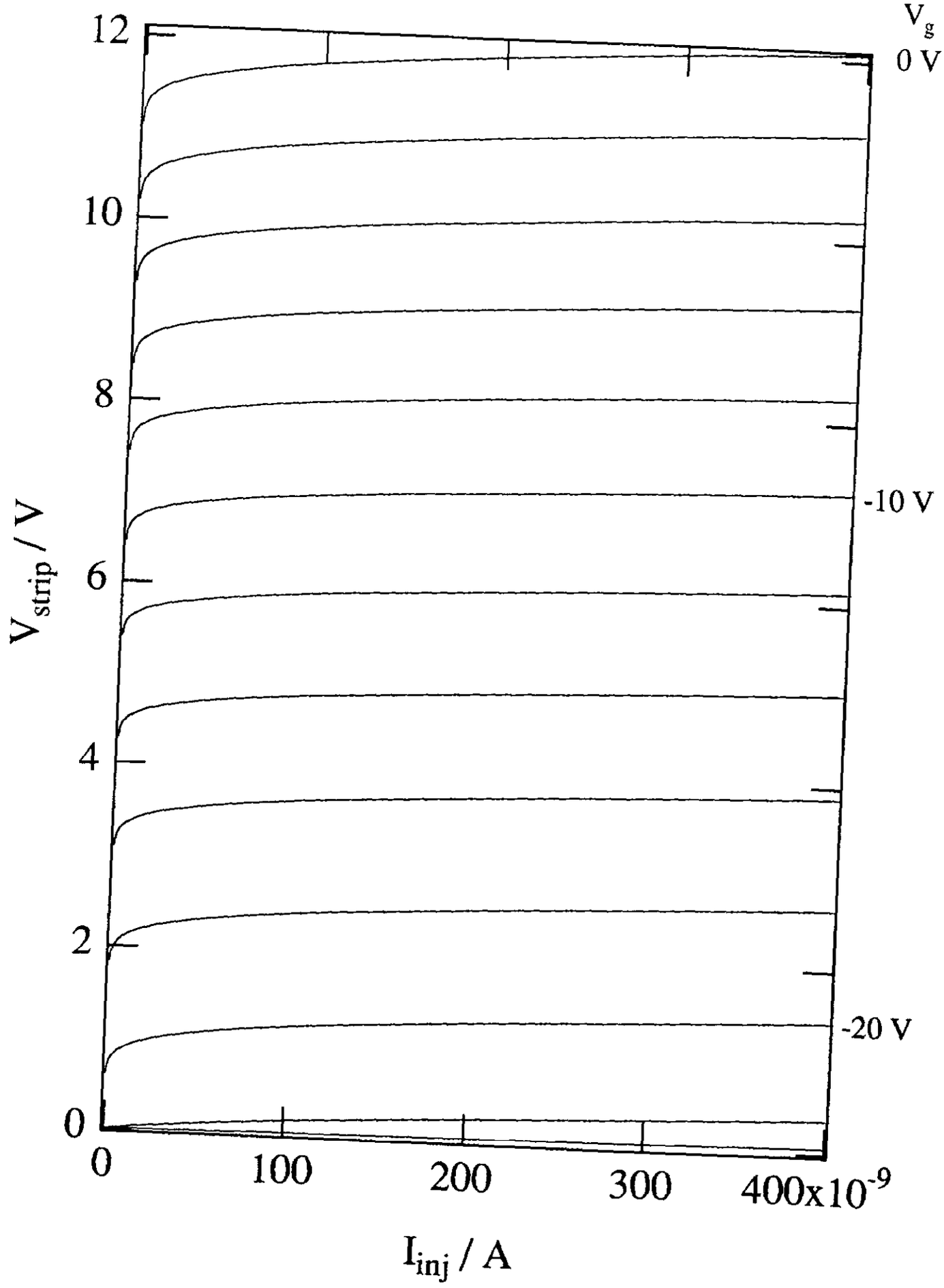

FIG. 5

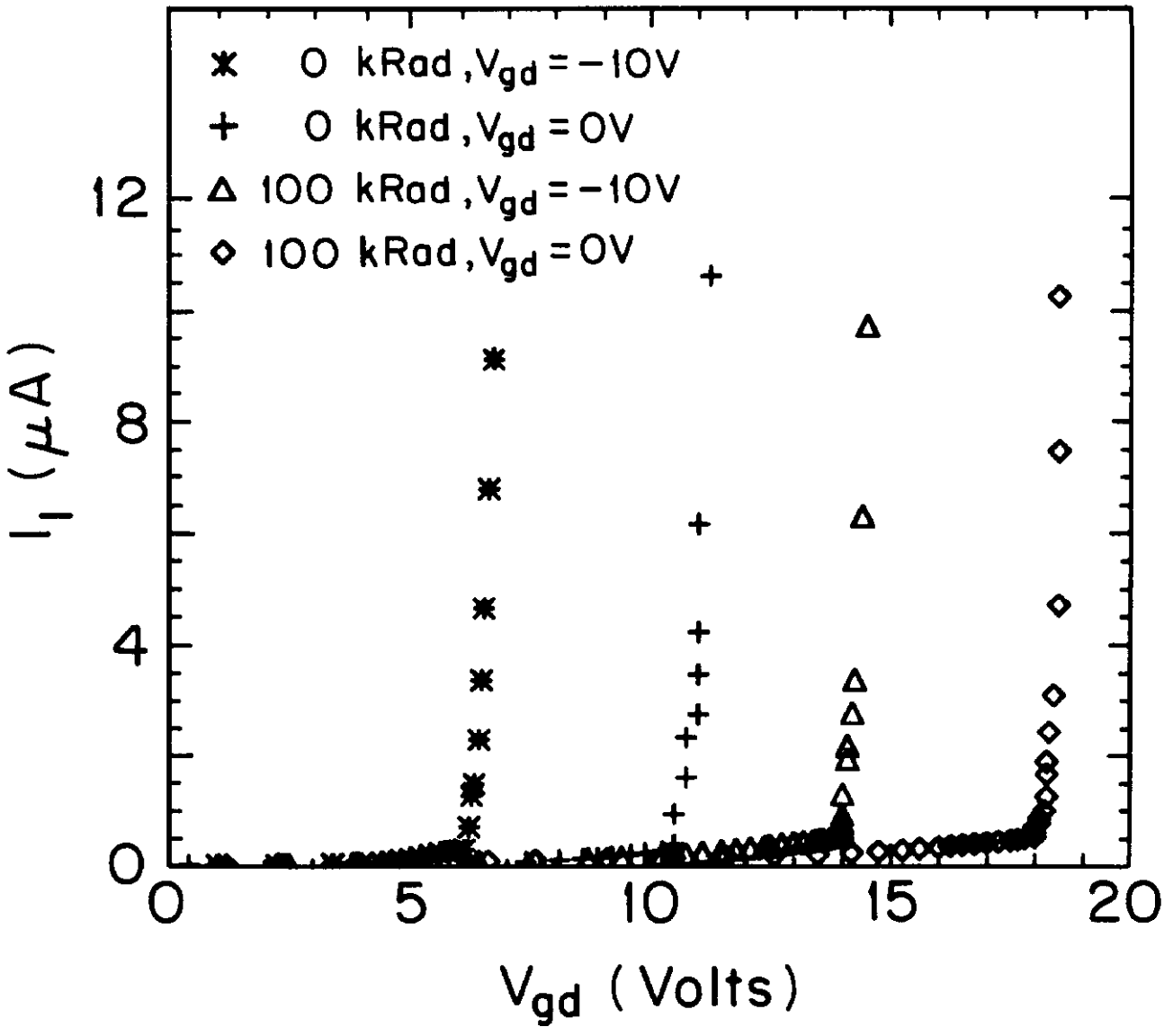
0 kRad, $V_{gd} = -10V$
0 kRad, $V_{gd} = 0V$
100 kRad, $V_{gd} = -10V$
100 kRad, $V_{gd} = 0V$
I_1 (μA)
0
4
8
12
0
5
10
15
20
V_{gd} (Volts)

FIG 3

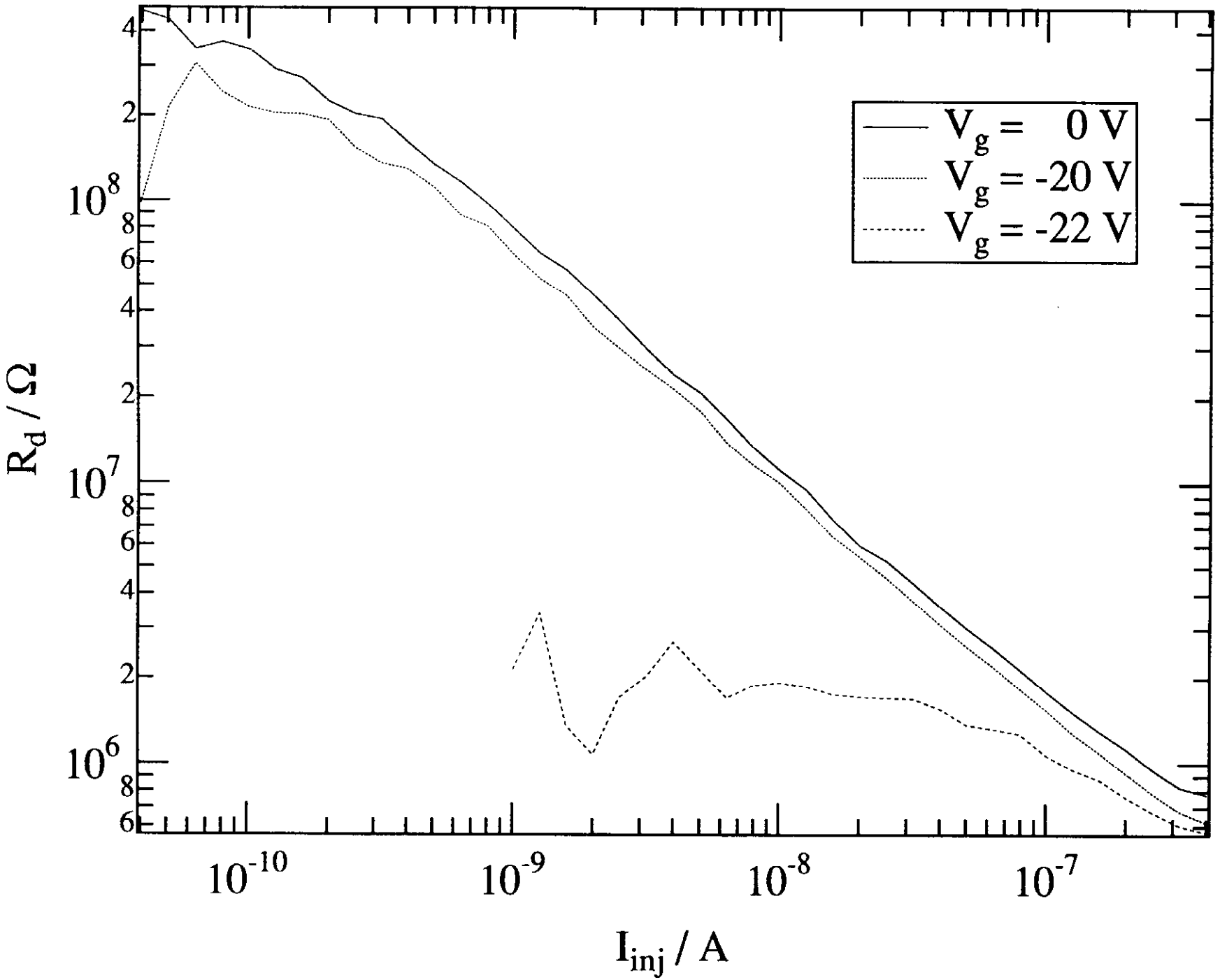

FIG. 7

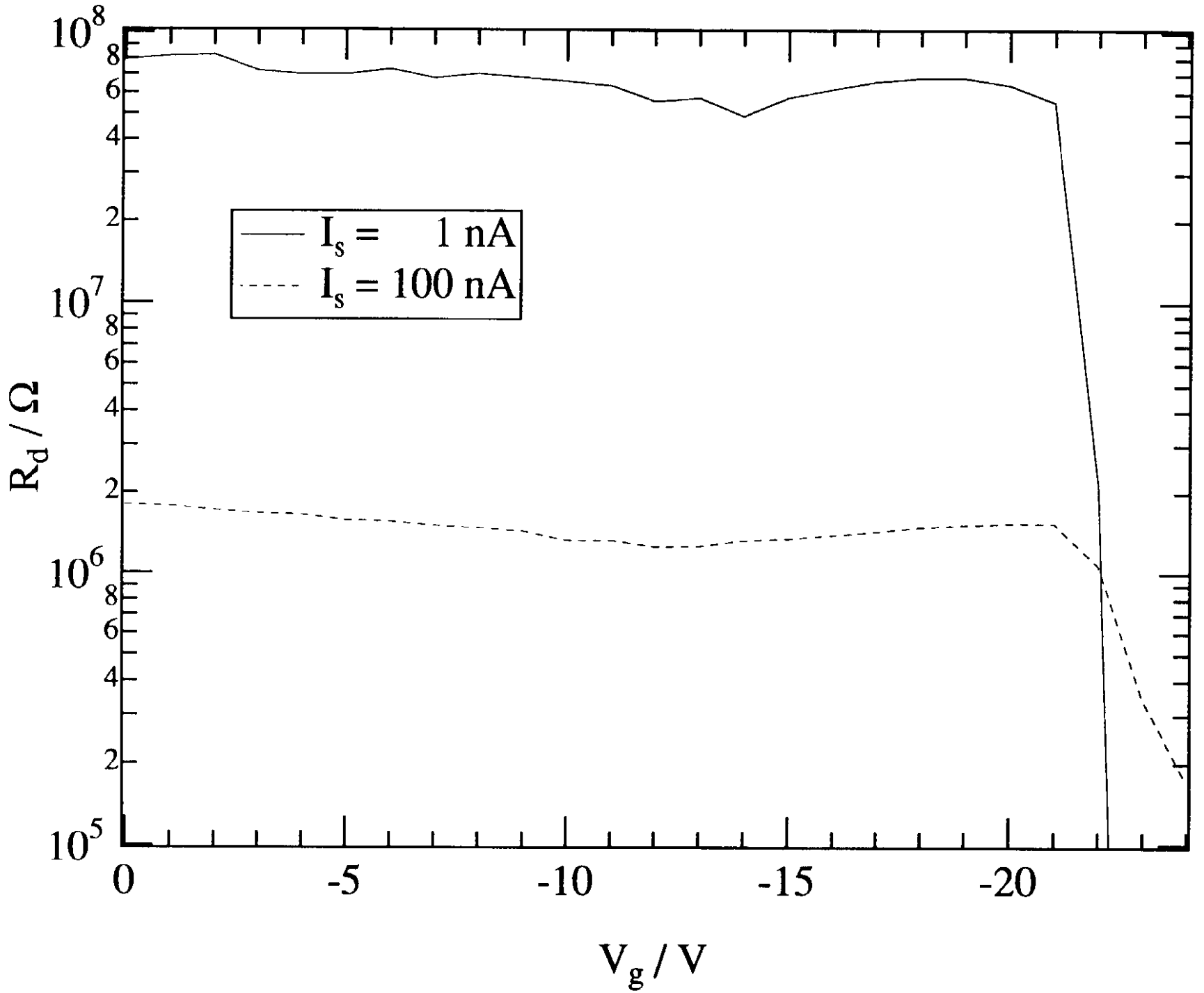
10^8
8
6
4
2
10^7
8
6
4
2
10^6
8
6
4
2
10^5
I_s = 1 nA
I_s = 100 nA
R_d / Ω
0
-5
-10
-15
-20
V_g / V

FIG. 8

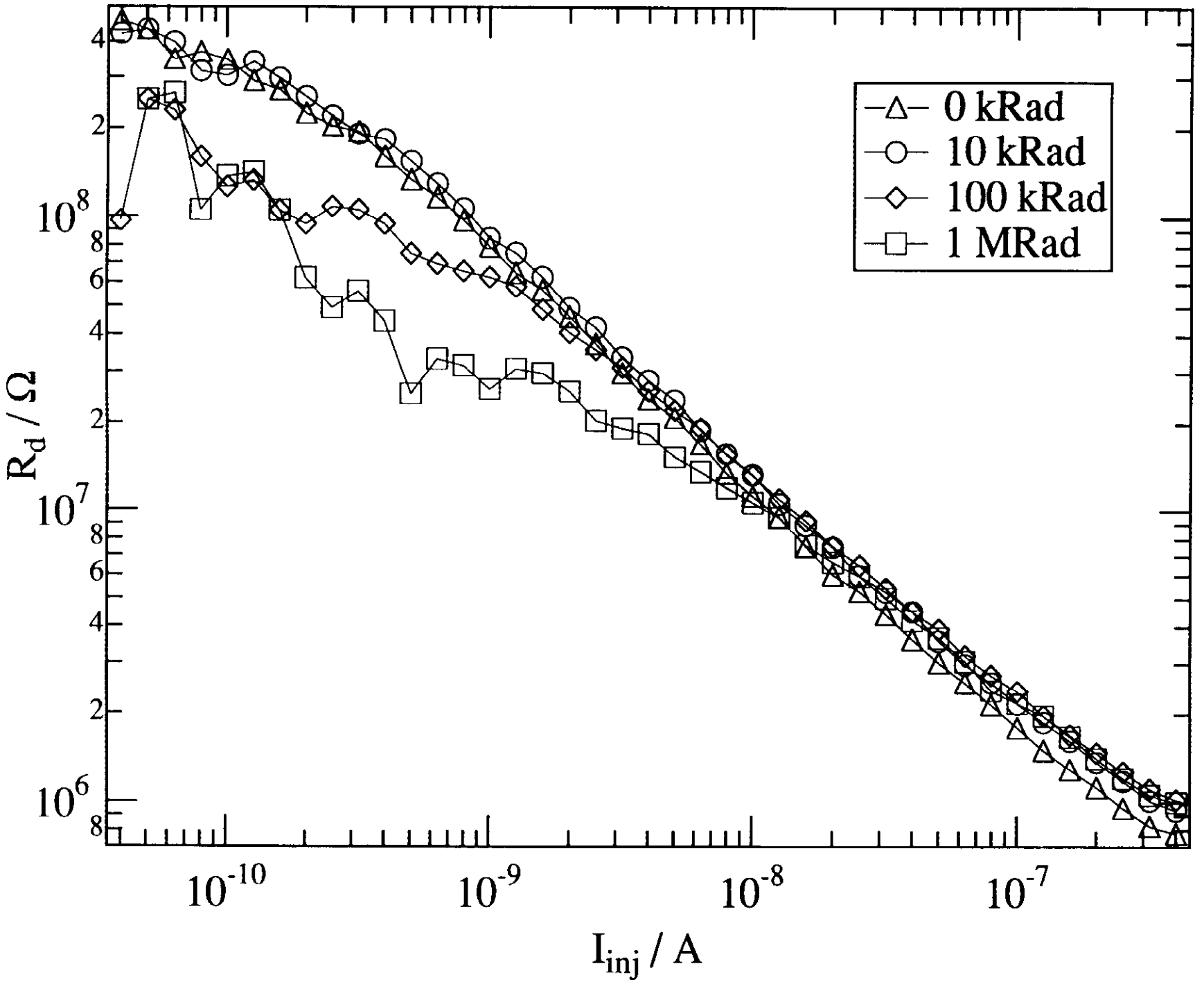
0 kRad
10 kRad
100 kRad
1 MRad
R_d / Ω
I_{inj} / A
10^{8}
10^{7}
10^{6}
10^{-10}
10^{-9}
10^{-8}
10^{-7}

FIG 9

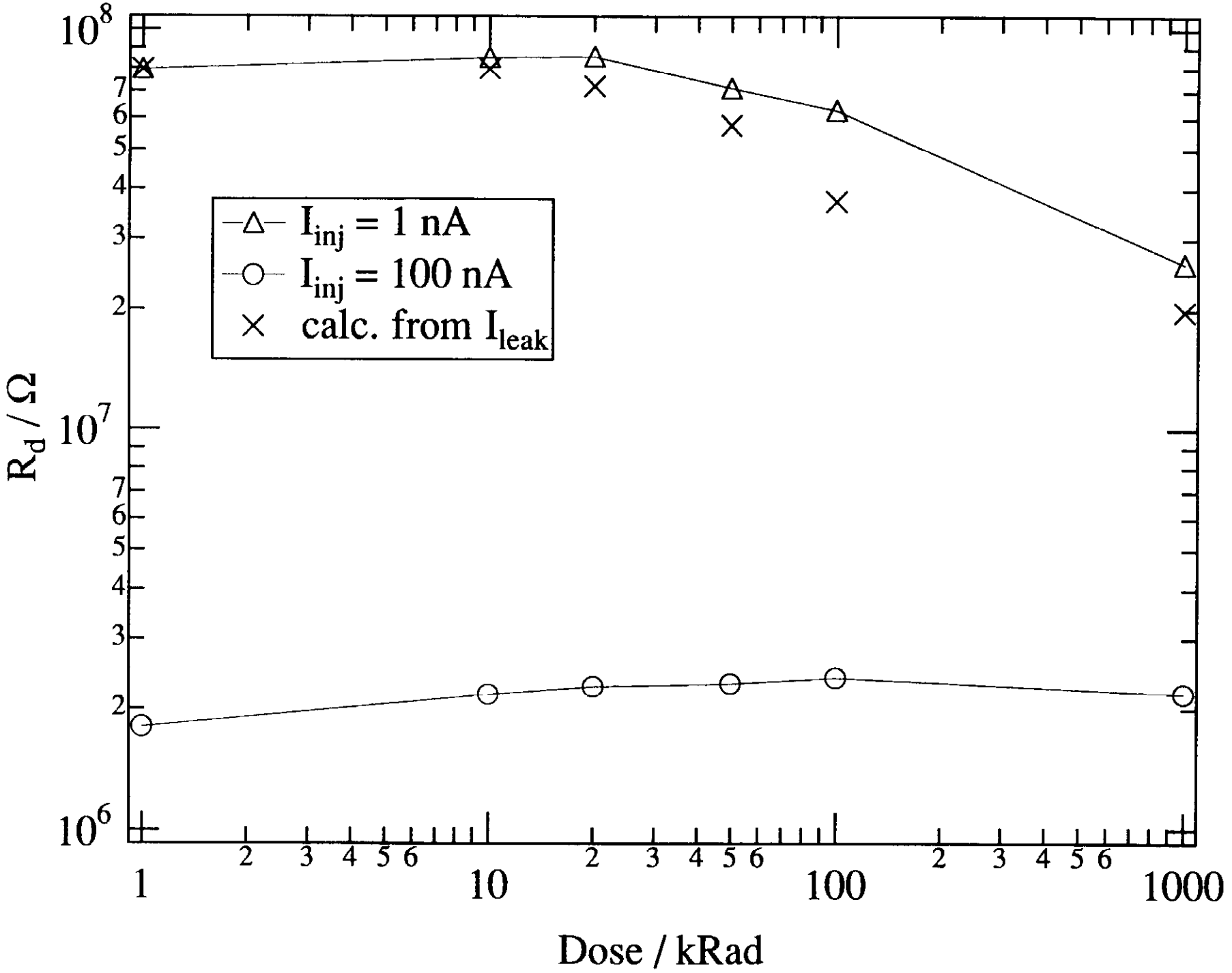
10^8
7
6
5
4
3
2
10^7
7
6
5
4
3
2
10^6
R_d / Ω
I_{inj} = 1 nA
I_{inj} = 100 nA
calc. from I_{leak}
1
2 3 4 5 6
10
2 3 4 5 6
100
2 3 4 5 6
1000
Dose / kRad

FIG. 10

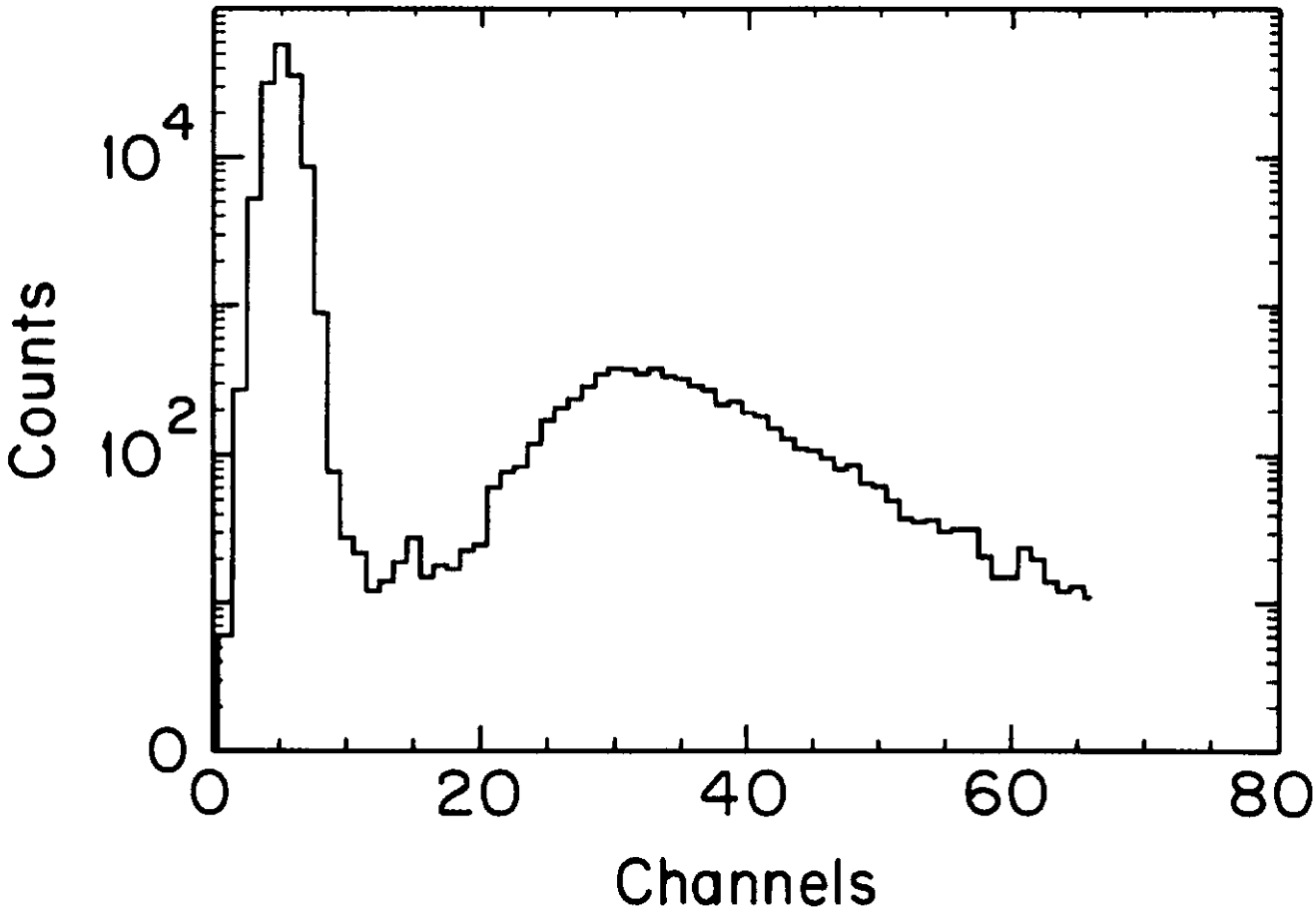

FIG. 1

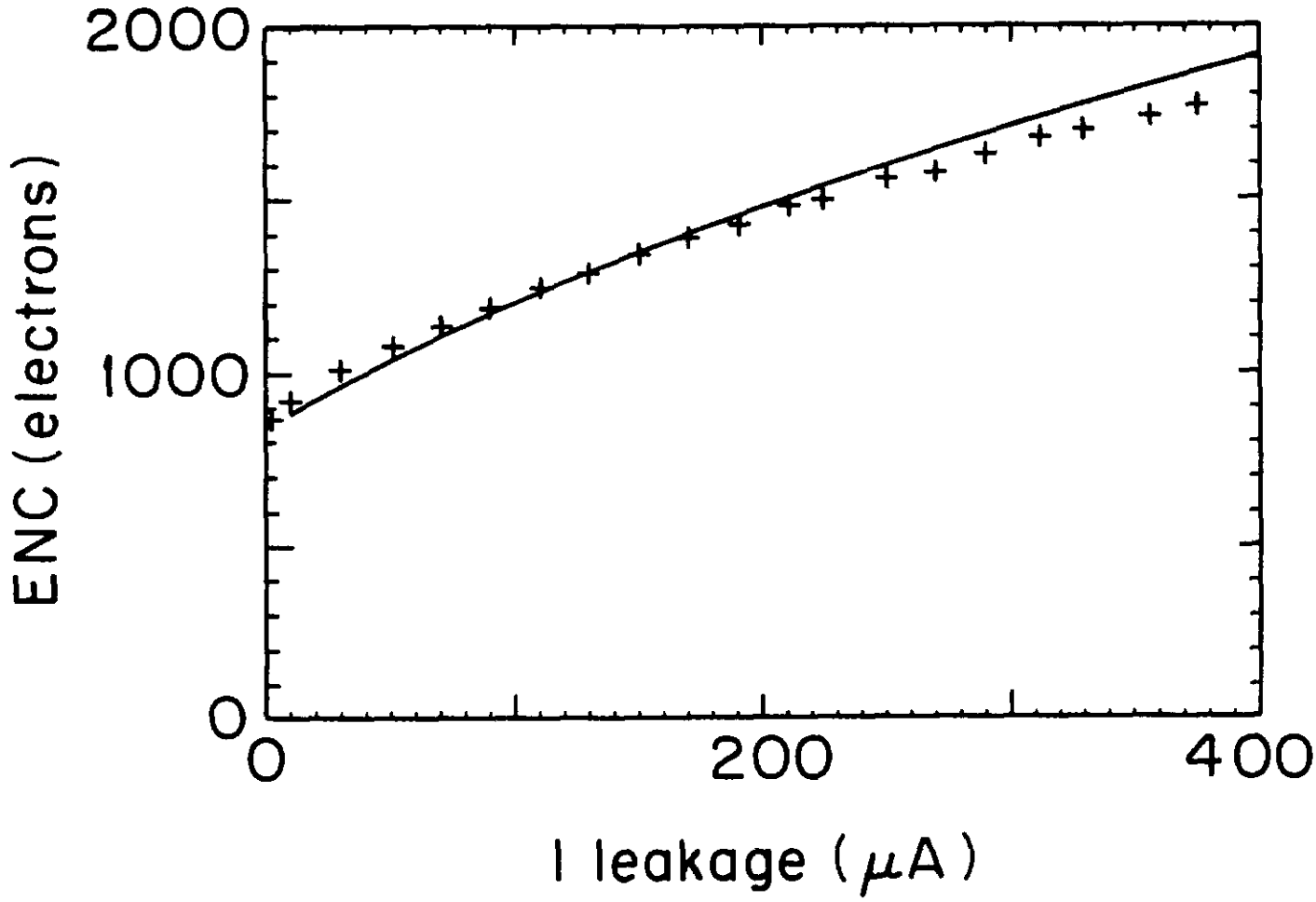

FIG 12

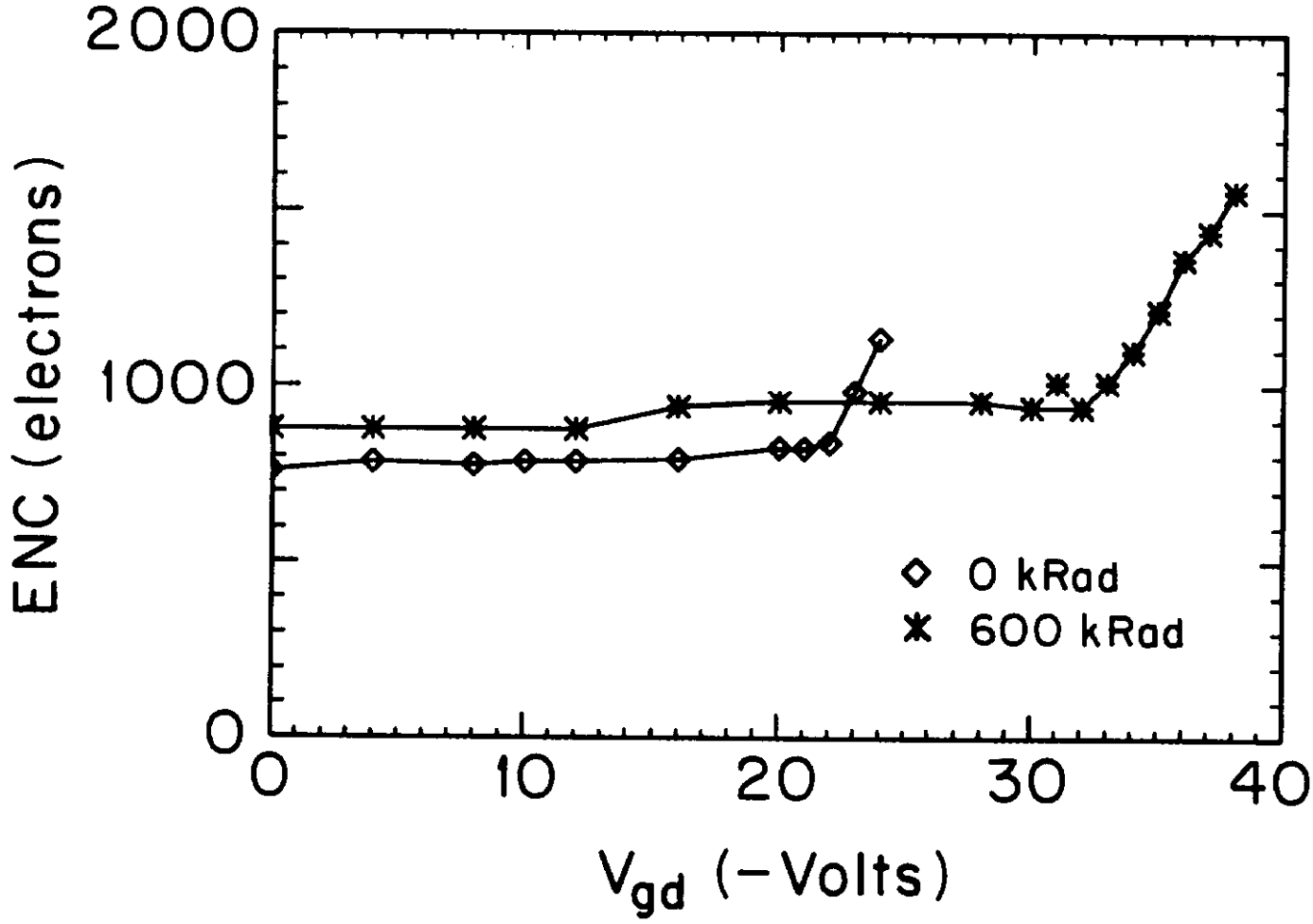
2000
1000
0
ENC (electrons)
0
10
20
30
40
V_{gd} (−Volts)
◇ 0 kRad
✱ 600 kRad

FIG. 13.